

Characterization of electron beams produced by ultrashort (30 fs) laser pulses

V. Malka, J. Faure, J. R. Marquès, and F. Amiranoff

LULI, UMR No. 7605, CNRS-CEA-Ecole Polytechnique-Université Pierre et Marie Curie, 91128 Palaiseau Cedex, France

J. P. Rousseau, S. Ranc, and J. P. Chambaret

Laboratoire d'Optique Appliquée, Ecole Nationale Supérieure des Techniques Avancées, 91128 Palaiseau, France

Z. Najmudin and B. Walton

Imperial College, London, United Kingdom

P. Mora and A. Solodov

Centre de Physique Théorique, CNRS-Ecole Polytechnique, 91128 Palaiseau Cedex, France

(Received 14 February 2001; accepted 30 March 2001)

Detailed measurements of electron spectra and charges from the interaction of 10 Hz, 600 mJ laser pulses in the relativistic regime with a gas jet have been done over a wide range of intensities (10^{18} – 2×10^{19} W/cm²) and electron densities (1.5×10^{18} – 1.5×10^{20} cm⁻³), from the “classical laser wakefield regime” to the “self-modulated laser wakefield” regime. In the best case the maximum electron energy reaches 70 MeV. It increases at lower electron densities and higher laser intensities. A total charge of 8 nC was measured. The presented simulation results indicate that the electrons are accelerated mainly by relativistic plasma waves, and, to some extent, by direct laser acceleration. © 2001 American Institute of Physics. [DOI: 10.1063/1.1374584]

Laser plasma interaction in the relativistic regime is crucial for laser plasma acceleration^{1–3} and for inertial confinement fusion (ICF) with the fast ignitor scheme.⁴ The success of these applications depends on the efficiency of the transfer of energy from the laser to electrons. On one hand, electrons can be trapped in high amplitude relativistic plasma waves (RPW) driven by the self-modulated laser wake field instability (SMLWF).^{5–7} In this relativistic regime plasma waves can reach amplitudes of a few tens of percent,^{8–10} accelerating electrons energies up to several tens of MeV.^{11,12} On the other hand, the measurement of multi-MeV electrons was recently imputed to direct laser acceleration in a plasma channel¹³ with an effective temperature deduced from electron spectra increasing with electron density.¹⁴

In this paper, we report on experimental electron generation in the SMLWF regime for ultrarelativistic laser pulses $a_0 > 1$, where a_0 is the normalized vector potential of the laser. For the first time, we observed that in our range of parameters: (i) the maximum electron energy increases when the electron density decreases in contrast with the results of Ref. 14; (ii) the maximum electron energy increases with the laser intensity. We show that the contribution to electron energy gain is due both to acceleration in relativistic plasma waves and to direct laser acceleration (DLA), again in contrast with the results of Ref. 14, where DLA was the dominant mechanism.

The experiment was performed at Laboratoire d'Optique Appliquée (LOA) with the titanium doped sapphire (Ti:Sa) laser¹⁵ operating at $\lambda_L = 0.82 \mu\text{m}$ in the chirped-pulse amplification (CPA) mode.¹⁶ In this configuration the laser delivered an energy up to 0.6 J (on target) in 35 fs full width half

maximum (FWHM) pulses with a linear polarization. The laser beam was focused onto the edge of a gas jet with an $f/7.5$ off-axis parabola. The laser distribution at full energy at the focal plane was a Gaussian function with a waist $w_0 = 6 \mu\text{m}$ containing 50% of the total laser energy. This corresponds to typical powers of 20 TW and to on-target intensities I_L of the order of 2×10^{19} W/cm². To avoid refraction induced by ionization processes,^{17,18} the laser beam was focused onto the sharp edge of a 2 mm diam laminar plume of helium gas from a pulsed, supersonic gas jet located 1 mm below the focal region. The flat top neutral density profile was characterized by interferometry.¹⁹

In this paper, we will focus our attention on electron measurements in the forward direction using an electron spectrometer. The electron spectrometer is able to measure electron energies from 0 to 200 MeV by changing the magnetic field value B from 0 to 1.5 T. A thick (4 cm) stainless steel piece with 1 cm internal diameter located at the entrance of the spectrometer was used as a collimator, giving a collection aperture of $f/100$. A vacuum box connected with the vacuum chamber was used in order to be able to measure the lower energy electrons. The spectra were measured with four biased silicon surfaced barrier detectors (SBD). A reference SBD detector was located along the laser axis after the electron spectrometer. Several null tests were done in order to make sure that the diode signals were really due to electrons. (i) Without magnetic field ($B=0$) the signal was greater than 1 V on the reference diode and no signal was recorded on the other diodes. (ii) With magnet on ($B>0$), the reference signal dropped to 10 mV while the electron signal on the other diodes increased. (iii) When changing the

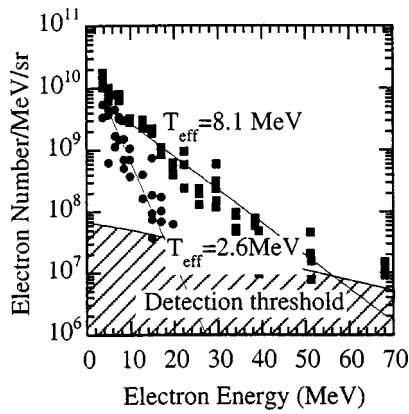


FIG. 1. Electron spectra measured at $1.5 \times 10^{20} \text{ cm}^{-3}$ (circles) and $5 \times 10^{19} \text{ cm}^{-3}$ (squares). Exponential fit with the deduced effective electron temperature.

value of B to get the same electron energy on another channel, the signal remained the same. Finally to confirm the value of the electron energy, we put copper pieces of different thicknesses and with a well-known stopping power in front of the diodes. The electrical noise on the detectors limited the sensitivity to about 100 electrons at 50 MeV.

We present in Fig. 1 two typical electron spectra obtained at $5 \times 10^{19} \text{ cm}^{-3}$ and $1.5 \times 10^{20} \text{ cm}^{-3}$. The laser parameters were 0.6 J and 35 fs. We observe that the distribution of electrons of energy above 4 MeV is well fitted by an exponential function, characteristic of an effective temperature for the electron beam. These effective temperatures are 8.1 MeV (2.6 MeV) for an electron density of $5 \times 10^{19} \text{ cm}^{-3}$ ($1.5 \times 10^{20} \text{ cm}^{-3}$). We can also deduce a typical value of 54 MeV (15 MeV) for the maximum electron energy. We observe an important decrease of the effective temperature and of the maximum electron energy when increasing the electron density.

This is summarized in Fig. 2, where we present the maximum electron energy vs the electron density. It decreases from 70 MeV to 15 MeV when the electron density increases from $1.5 \times 10^{19} \text{ cm}^{-3}$ to $1.5 \times 10^{20} \text{ cm}^{-3}$. First, we can compare the maximum electron energy to the one due to

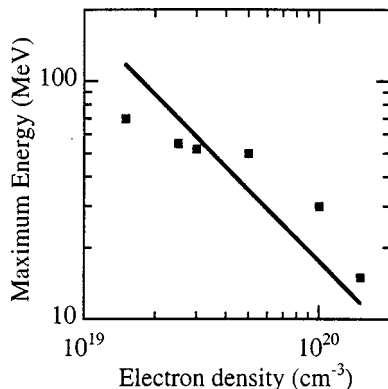


FIG. 2. Maximum electron energy as a function of the electron density. Squares correspond to experimental values. The continuous line corresponds to theoretical calculation with a normalized electrostatic field $E_z/E_0=0.5$. Laser parameters: 0.6 J, 35 fs, and $2 \times 10^{19} \text{ W/cm}^2$.

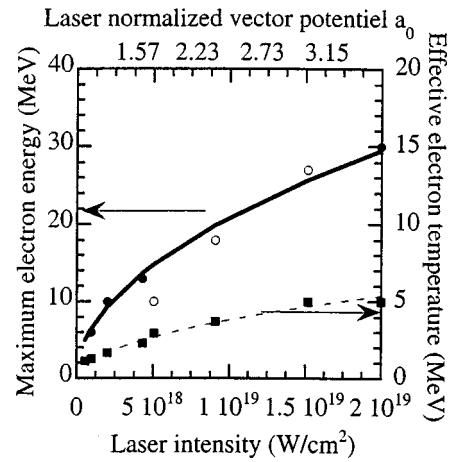


FIG. 3. Maximum electron energy (left scale, circles) and electron temperature (right scale, squares) as a function of the laser intensity at 10^{20} cm^{-3} obtained by changing the laser energy (empty circles) with a 35 fs laser pulse and by changing the pulse duration (dark circles) with a 0.6 J laser energy. The continuous line corresponds to the scaling law, $E_{\text{max}}(\text{MeV}) = 6.6I_{18}^{1/2}$ for the maximum electron and the dashed line corresponds to $T(\text{MeV}) = 1.2I_{18}^{1/2}$ for the electron temperature.

acceleration in relativistic plasma waves with a constant amplitude. This energy is equal to the product of the electrostatic field by an optimum length. This length is the dephasing length and corresponds to exactly half a wavelength in the wave frame,²⁰ $W_{\text{max}} \approx 4\gamma_p^2(E_z/E_0)mc^2$, where γ_p is the plasma wave Lorentz factor (which is equal to the square root of the critical density to electron density ratio n_c/n_e) and E_z/E_0 is the electrostatic field normalized to $E_0 = c m \omega_p / e$. Presented in Fig. 2 is the theoretical value deduced from this equation for a given value of the normalized electrostatic field $E_z/E_0=0.5$. Nonlinear corrections due to the effect of a relativistic pump, to self-channeling²¹ and to the reduction of the phase velocity of plasma waves³ have been neglected. Experimental results are in reasonable agreement with this model. For electron densities greater than $1.5 \times 10^{19} \text{ cm}^{-3}$ the maximum electron energy varies as $E_{\text{max}}(\text{MeV}) = 0.76 n_c/n_e$.

We present in Fig. 3 the maximum electron energy as a function of the laser intensity obtained by changing the laser energy or the pulse duration, at a fixed density of 10^{20} cm^{-3} . Increasing the laser energy from 0.15 J to 0.6 J increases a_0 from 1.58 to 3.15. Changing the laser pulse duration from 630 fs to 35 fs, a_0 varies from 0.74 to 3.15. We observe that the maximum electron energy increases from 6 MeV to 30 MeV when the laser intensity increases from $1.0 \times 10^{18} \text{ W/cm}^2$ to $2.0 \times 10^{19} \text{ W/cm}^2$ approximately as the square root of the laser intensity, $E_{\text{max}}(\text{MeV}) = 6.6I_{18}^{1/2}$, where $I_{18} = 10^{18} \text{ W/cm}^2$. In Fig. 3 we also present the electron temperature as a function of the laser intensity. The electron temperature also increases with the square root of the laser intensity, $T(\text{MeV}) = 1.2I_{18}^{1/2}$. This result is in agreement with the numerical result obtained by Pukhov¹³ for a plasma with an exponential density profile. Although the acceleration in plasma waves gives the correct behavior for the variation of the maximum energy as a function of the elec-

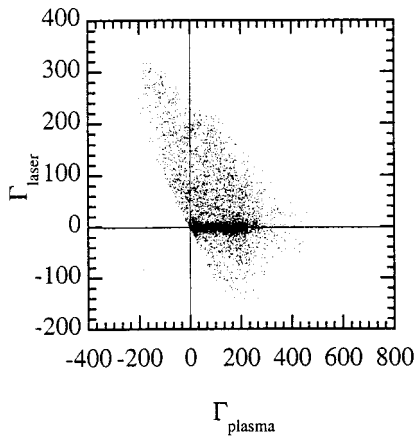


FIG. 4. Distribution of the accelerated test electrons in the (Γ_p, Γ_l) space in the simulation for a 0.6 J laser pulse propagating in a plasma of electron density $2 \times 10^{19} \text{ cm}^{-3}$.

tron density, one cannot exclude the possibility of direct laser acceleration.

To get an insight into the acceleration mechanisms, we also performed numerical simulations of the laser pulse propagation in a plasma using the axisymmetric fully-relativistic particle code Wake.²² Due to the approximations used in the code we were limited to the case of laser powers less than a few critical powers for relativistic self-focusing. For the maximum laser energy of the present experiment, it corresponds to electron densities up to $2 \times 10^{19} \text{ cm}^{-3}$. We also made simulations with larger densities but with smaller powers. Simulations of electron acceleration were performed by pushing test (noninteracting) electrons in the field regions at the time of strong self-focusing for short pulses and at the developed stage of self-modulation for laser pulses longer than a plasma period. Beam loading effects²³ are absent in the present approach which along with the axisymmetric constraint could overestimate the wakefield amplitude and the electron acceleration. However the results of the simulations confirm qualitatively the decrease of the maximum electron energy with the increase of the background electron density when the length over which self-focusing occurs is greater than the dephasing length. In our simulations one can separate the effect of the laser field and of the plasma wave field, which both contain transverse and longitudinal components. To compare these effects we calculated the integrals,

$$\Gamma_{p,l} = - \int_0^t \frac{e \mathbf{E}_{p,l} \cdot \mathbf{v}}{mc^2} dt'$$

along the test electrons trajectories. $\Gamma_{p,l}$ represents the energy gain due to plasma wake field and laser field, respectively (note that our integrals Γ_p and Γ_l are different from the quantities Γ_z and Γ_{\perp} by Gahn *et al.*,¹⁴ who used $\mathbf{E} \cdot \mathbf{p}$ instead of $\mathbf{E} \cdot \mathbf{v}$ and separated \mathbf{E} in E_z and \mathbf{E}_{\perp} instead of \mathbf{E}_p and \mathbf{E}_l). In Fig. 4 we show the distribution of the accelerated electrons in the (Γ_p, Γ_l) space after the full length of acceleration in a typical simulation. This simulation corresponds to the present experiment with a 0.6 J laser pulse propagating in a plasma of electron density $2 \times 10^{19} \text{ cm}^{-3}$. The bunch of 3×10^4 test electrons was injected after one Rayleigh length

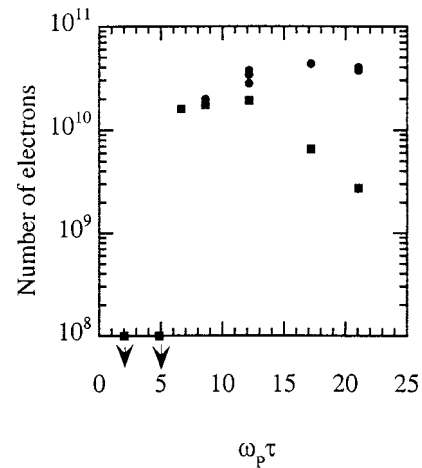


FIG. 5. Total electron number (circles) and number of electrons with energies greater than 3.7 MeV (squares) as a function of the product $\omega_p \tau$, where ω_p is the plasma frequency and τ is the laser pulse duration (35 fs).

of the laser pulse propagation in plasma. While we confirm the importance of direct laser acceleration¹³ we find out that the most energetic electrons still come from the acceleration by the plasma wave field in this simulation. We note, as the length of the pulse propagation is larger than the dephasing length, that a part of the energetic electrons is decelerated by the plasma wake. At the same time we find that as in vacuum,²⁴ the longitudinal component of the laser field implied by $\nabla \cdot \mathbf{E} = 0$ strongly reduces the efficiency of the direct laser acceleration mechanism at the betatron resonance.¹³ However for higher plasma densities, the laser pulse is much longer than a plasma period with powers much greater than the critical power for self-focusing, and most energetic electrons could come from the direct laser acceleration.¹³

We have also measured the total charge with an integrated charge transformer as a function of the electron density, fixing the pulse duration at 35 fs. The result is plotted in Fig. 5 as a function of $\omega_p \tau$ (ω_p is the plasma frequency and τ is the pulse duration), from the wakefield regime ($\omega_p \tau \approx 2$) to the self-modulated regime ($\omega_p \tau > 2$). Near the wakefield regime no electrons were detected, whereas with increasing $\omega_p \tau$ the number of electrons increased. At higher electron density the number of electrons with energy greater than 3.7 MeV and detected by the spectrometer became smaller than those measured with the charge collector because the radial wake scattered electrons out of the aperture cone of the electron spectrometer. The total charge is about 8 nC in agreement with recent numerical simulations,^{13,25} whereas the charge for electrons with energies greater than 3.7 MeV is about 1 nC.

In conclusion we have measured electron spectra (with energy up to 70 MeV) and electron beam charge (greater than 5 nC) over a wide range of electron density and laser intensity. The maximum electron energy increases when the density decreases, and at a given electron density it increases when the laser intensity increases. In the low density regime, numerical simulations indeed show that electrons are mainly accelerated by self-modulated laser wakefield instability. The discrepancy with the results of Ref. 14 with respect to the

dependence of the electron energy spectrum with the electron density might be due to the laser parameters (shorter and more energetic pulses in our case) and to the use of a supersonic gas jet. As opposed to a subsonic gas jet which produces nonuniform plasmas,¹⁴ a supersonic gas jet produces uniform plasmas in which the self-modulated laser wakefield instability can be easily driven.

ACKNOWLEDGMENT

The work of A.S. was supported in part by the Russian Basic Research Foundation (Grant No. 98-02-17205, 99-02-16399).

¹T. Tajima and J. Dawson, Phys. Rev. Lett. **43**, 267 (1979).

²A. Modena, A. E. Dangor, Z. Najmudin *et al.*, Nature (London) **377**, 606 (1995).

³E. Esarey, P. Sprangle, J. Krall *et al.*, IEEE Trans. Plasma Sci. **24**, 252 (1996).

⁴M. Tabak, J. Hammer, M. E. Glinsky *et al.*, Phys. Plasmas **1**, 1626 (1994).

⁵N. E. Andreev, L. M. Gorbunov, V. I. Kirsanov *et al.*, JETP Lett. **55**, 571 (1992).

⁶T. M. Antonsen and P. Mora, Phys. Rev. Lett. **69**, 2204 (1992).

⁷P. Sprangle, E. Esarey, J. Krall *et al.*, Phys. Rev. Lett. **69**, 2200 (1992).

⁸C. E. Clayton, D. Gordon, K. A. Marsh *et al.*, Phys. Rev. Lett. **81**, 100 (1998).

⁹A. Ting, C. I. Moore, K. Krushelnick *et al.*, Phys. Rev. Lett. **77**, 5377 (1996).

¹⁰S. P. LeBlanc, M. C. Downer, R. Wagner *et al.*, Phys. Rev. Lett. **77**, 5381 (1996).

¹¹D. Gordon, K. C. Tzeng, C. E. Clayton *et al.*, Phys. Rev. Lett. **80**, 2133 (1998).

¹²C. I. Moore, A. Ting, K. Krushelnick *et al.*, Phys. Rev. Lett. **79**, 3909 (1997).

¹³A. Pukhov, Z. M. Sheng, and J. Meyer-ter-Vehn, Phys. Plasmas **6**, 2847 (1999).

¹⁴C. Gahn, G. Tsakiris, A. Pukhov *et al.*, Phys. Rev. Lett. **83**, 4772 (1999).

¹⁵A. Antonetti, F. Blasco, J. P. Chambaret *et al.*, Appl. Phys. B: Lasers Opt. **65**, 197 (1997).

¹⁶D. Strickland and G. Mourou, Opt. Commun. **56**, 219 (1985).

¹⁷V. Malka, E. D. Wispelaere, J. R. Marquès *et al.*, Phys. Plasmas **3**, 1682 (1996).

¹⁸P. Monot, thèse de doctorat de l'Université Paris-sud, Centre d'Orsay, 1993.

¹⁹V. Malka, C. Coulaud, J. P. Geindre *et al.*, Rev. Sci. Instrum. **71**, 2329 (2000).

²⁰P. Mora and F. Amiranoff, J. Appl. Phys. **66**, 3476 (1989).

²¹E. Esarey, B. Hafizi, R. Hubbard *et al.*, Phys. Rev. Lett. **80**, 5552 (1998).

²²P. Mora and T. M. Antonsen, Phys. Plasmas **4**, 217 (1997).

²³T. Katsouleas, S. Wilks, P. Chen *et al.*, Part. Accel. **22**, 81 (1987).

²⁴B. Quesnel and P. Mora, Phys. Rev. E **58**, 3719 (1998).

²⁵K. C. Tzeng, W. B. Mori, and T. Katsouleas, Phys. Plasmas **6**, 2105 (1999).